



**HAL**  
open science

## Influence of the properties of 7 micro-grain activated carbons on organic micropollutants removal from wastewater effluent

Ronan Guilloso, Julien Le Roux, Romain Mailler, Catherine Morlay, Emmanuelle Vulliet, Fabrice Nauleau, Vincent Rocher, Johnny Gasperi

### ► To cite this version:

Ronan Guilloso, Julien Le Roux, Romain Mailler, Catherine Morlay, Emmanuelle Vulliet, et al.. Influence of the properties of 7 micro-grain activated carbons on organic micropollutants removal from wastewater effluent. *Chemosphere*, 2020, 243, pp.125306. 10.1016/j.chemosphere.2019.125306 . hal-02394590

**HAL Id: hal-02394590**

**<https://enpc.hal.science/hal-02394590v1>**

Submitted on 28 Jun 2020

**HAL** is a multi-disciplinary open access archive for the deposit and dissemination of scientific research documents, whether they are published or not. The documents may come from teaching and research institutions in France or abroad, or from public or private research centers.

L'archive ouverte pluridisciplinaire **HAL**, est destinée au dépôt et à la diffusion de documents scientifiques de niveau recherche, publiés ou non, émanant des établissements d'enseignement et de recherche français ou étrangers, des laboratoires publics ou privés.

1 **Title**

2 Influence of the properties of 7 micro-grain activated carbons on organic micropollutants removal from  
3 wastewater effluent

4 **Authors**

5 Ronan Guillosoy<sup>1\*</sup>, Julien Le Roux<sup>1</sup>, Romain Mailler<sup>2</sup>, Catherine Morlay<sup>3</sup>, Emmanuelle Vulliet<sup>4</sup>, Fabrice  
6 Nauleau<sup>5</sup>, Vincent Rocher<sup>2</sup>, Johnny Gasperi<sup>1</sup>

7 <sup>1</sup> Ecole des Ponts ParisTech, Université Paris-Est Créteil, AgroParisTech, Laboratoire Eau Environnement et  
8 Systèmes Urbains, UMR MA 102, Créteil, France

9 <sup>2</sup> Service public de l'assainissement francilien (SIAAP), Direction Innovation et Environnement, Colombes,  
10 France

11 <sup>3</sup> Université de Lyon, CNRS, Université Claude Bernard Lyon 1, INSA-Lyon, MATEIS, UMR 5510,  
12 Villeurbanne, France

13 <sup>4</sup> Université de Lyon, CNRS, Université Claude Bernard Lyon 1, Institut des Sciences Analytiques, UMR  
14 5280, Villeurbanne, France

15 <sup>5</sup> Saur, Direction de la Recherche et du Développement, Maurepas, France

16 \* Corresponding author: ronan.guillossou@enpc.fr

17 **Highlights**

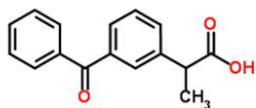
- 18 • 7 commercial  $\mu$ GACs were characterized and tested with real wastewater  
19 • A percentage of microporous volume higher than 65% reduced OMPs adsorption  
20 • DOM reduced the adsorption of negatively-charged OMPs more than positive ones  
21 • OMPs charge, hydrophobicity and minimal projection area influenced their adsorption  
22 • The  $\mu$ GACs particle size had an impact on  $UV_{254}$  removal in continuous column tests

23 **Graphical abstract**

## 7 newly commercialized micro-grain activated carbons for wastewater advanced treatment



### Key properties for micropollutants removal



Microporous volume  
Particle size  
Point of zero charge



24

### 25 Abstract

26 Most studies dedicated to organic micropollutants (OMPs) removal from wastewater effluents by adsorption  
27 onto activated carbon (AC) only consider a few conventional AC properties. The link between OMPs removal  
28 and these properties is often missing, which limits the understanding of the adsorption process and the  
29 interpretation of the results. The chemical, physical and textural properties of seven newly commercialized  
30 micro-grain activated carbons ( $\mu$ GACs) were determined to assess their influence on the removal of 28 OMPs.  
31 Conventional batch tests with wastewater effluent showed that a high percentage of microporous volume (>  
32 65%) was detrimental for the removal of 10 OMPs, probably due to a higher blockage of micropores by  
33 dissolved organic matter (DOM). The removal of 5 OMPs was correlated with  $\mu$ GACs surface chemistry  
34 properties (i.e. charge) which were potentially modified by DOM adsorption or inorganic species, thus  
35 favoring the adsorption of positively-charge compounds. A combination of OMPs properties including their  
36 charge, hydrophobicity and minimal projection area could explain their removal. Correlations were found  
37 between the removal of several OMPs and UV<sub>254</sub> and dissolved organic carbon, suggesting that DOM and  
38 OMPs interacted with each other or followed similar adsorption mechanisms. A decrease in  $\mu$ GACs particle  
39 size had a positive impact on UV<sub>254</sub> removal under continuous-flow conditions in columns representative of a  
40 large-scale pilot due to better expansion.

### 41 Keywords

42 Wastewater advanced treatment; Organic micropollutants; Adsorption; Micro-grain activated carbon.

### 43 1. Introduction

44 Advanced processes from the drinking water industry have been increasingly transferred to wastewater  
45 treatment plants to find an adequate technology for organic micropollutants (OMPs) removal, and activated  
46 carbon (AC) adsorption is a promising solution as it is easy to use, flexible and doesn't produce byproducts as  
47 compared to oxidation processes (Bui et al., 2016). Two types of ACs are commonly employed for drinking  
48 water production and advanced wastewater treatment: powdered activated carbon (PAC) and granular  
49 activated carbon (GAC). PAC, with particle sizes smaller than 100  $\mu\text{m}$ , can be used in conventional processes  
50 (Streicher et al., 2016) or in contact reactors followed by a separation step (i.e. membrane filtration or  
51 coagulation/flocculation) (Mailler et al., 2015; Margot et al., 2013). GAC, with particle sizes higher than 800  
52  $\mu\text{m}$ , is used in fixed bed filters (Benstoem et al., 2017; Ek et al., 2014; Paredes et al., 2016). Emerging types  
53 of ACs have been studied in recent years, such as micro-grain activated carbon ( $\mu\text{GAC}$ ) with a particle size  
54 ranging from 100 to 800  $\mu\text{m}$  (Alves et al., 2018; Guillosoy et al., 2019; Mailler et al., 2016a).  $\mu\text{GAC}$ s have  
55 the advantages of being regenerable like GACs and easily fluidized like PACs but without the need of a  
56 separation step. The properties of  $\mu\text{GAC}$ s are however poorly documented, especially in conjunction with  
57 their performances in terms of OMPs removal.

58 The adsorption of OMPs onto AC is a complex process that depends on many factors, including the chemical,  
59 physical and textural characteristics of the AC. These characteristics include particle density and size, surface  
60 area, pores sizes, pore volume distribution (micro-, meso- or macropores) and the presence of surface  
61 functional groups. Raposo et al. (2009) studied the adsorption of methylene blue on 3 GACs with 5 different  
62 particle sizes and found a decrease in methylene blue adsorption with an increase in particle size. The decrease  
63 in particle size allows, for an identical activated carbon mass, an increase of the available external surface area  
64 and thus facilitates the access to adsorption sites for OMPs. The particle size also influences AC expansion in  
65 fluidized bed reactors. An excessive expansion can lead to mass loss whereas an insufficient expansion  
66 increases the energy consumption and decreases the mass transfer (Bello et al., 2017).

67 The adsorption capacity depends on both textural and chemical characteristics of the AC. Mailler et al. (2016b)  
68 observed that the efficiency of 4 PACs was linked to their specific surface (Brunauer-Emmett-Teller, BET)  
69 which could be estimated from bulk density measurement. Contrarily, Benstoem and Pinnekamp (2017)  
70 showed that the BET surface was not correlated with the removal of 3 OMPs by 5 GACs. The iodine number  
71 and the methylene blue number were not correlated with the removal of OMPs, but a good correlation was

72 observed with the apparent density. Moreover, Zietzschmann et al. (2014a) found that the BET surface and  
73 the iodine number of 8 PACs were not correlated with the removal of 7 OMPs. The pore size and the pore  
74 volume distributions of the AC also have an impact since the adsorption energy value is related to the pore  
75 size relatively to the size of the adsorbate (Hsieh and Teng, 2000). OMPs are preferentially adsorbed onto  
76 high-energy adsorption sites which are primarily located in the smallest pores accessible (Quinlivan et al.,  
77 2005). The average micropore size is a key parameter for OMPs removal because the largest OMPs can be  
78 subjected to size exclusion from the narrowest micropores (Li et al., 2002; Yu et al., 2012). Alves et al. (2018)  
79 studied the removal of 23 pharmaceuticals onto 6  $\mu$ GACs and found that their textural properties played the  
80 most important role in the adsorption process in ultrapure water. The mesoporous volume was better correlated  
81 with OMPs removal than the microporous volume. Some authors observed that a low mesoporous volume is  
82 problematic for OMPs adsorption because of a possible pore blockage in the presence of DOM which is  
83 preferentially adsorbed onto mesopores and large micropores (Li et al., 2003; Newcombe et al., 2002b).  
84 Mesopores play a key role by adsorbing DOM and preventing micropores blockage which would further limit  
85 OMPs removal.

86 The surface chemistry of ACs (i.e. the presence of heteroatoms) leads to the presence of acidic and/or basic  
87 functional groups which may influence OMPs adsorption (Karanfil et al., 1996; Li et al., 2002). The AC  
88 surface can be charged due to protonation or deprotonation of these functional groups, and the point of zero  
89 charge ( $\text{pH}_{\text{pzc}}$ ) is defined as the pH value of the solution required to give a zero net surface charge. It is an  
90 important parameter controlling the electrostatic interactions between DOM, OMPs and the AC (Newcombe,  
91 1994; Yu et al., 2012). Alves et al. (2018) observed that in the presence of wastewater effluent, the surface  
92 chemistry of  $\mu$ GACs had more influence than textural properties due to the adsorption of DOM which  
93 modified  $\mu$ GACs surface chemistry. The presence of acidic functional groups (e.g. carboxylic acids, phenols,  
94 lactones) can also lead to the formation of water molecule clusters that can cause pore blockage and  
95 consequently prevent OMPs removal (Delgado et al., 2014; Li et al., 2002; Quinlivan et al., 2005).

96 Many studies have been carried out about the characterization of AC and the influence of their characteristics  
97 on the adsorption of OMPs, but most of the time only a limited number of OMPs were studied (Delgado et al.,  
98 2014; Yu et al., 2008), or experimental conditions were far from those of wastewater treatment facilities (e.g.  
99 in deionized/ultra-pure water) (Li et al., 2002; Yu et al., 2008). On the other hand, studies have been conducted

100 in advanced wastewater treatment facilities or in laboratory with real wastewater effluents, but AC  
101 characteristics are often lacking which limits the interpretation of the results (Benstoem et al., 2017; Margot  
102 et al., 2013).

103 The aim of this study was to fully characterize seven newly commercialized  $\mu$ GACs and to assess the influence  
104 of their properties on OMPs adsorption. First, a large diversity of chemical, physical and textural properties  
105 of the  $\mu$ GACs were determined. Then, conventional batch tests were conducted to determine the removal of  
106 28 OMPs from a real wastewater effluent. A statistical analysis was assessed to explore possible correlations  
107 existing between the chemical, physical and textural properties of the  $\mu$ GACs and OMPs removal. The  
108 properties of OMPs (e.g. charge, hydrophobicity and minimal projection area) were also considered to  
109 understand their removal. Finally, column tests were conducted in the laboratory under operative conditions  
110 that can be considered as representative of a large-scale pilot (i.e. continuous-flow mode, fluidized bed and  
111 similar carbon/flow ratio) to estimate bed expansion and optimal ascending velocity. Breakthrough curves of  
112 UV absorbance at 254 nm ( $UV_{254}$ ) were obtained for each  $\mu$ GAC to assess whether simple column tests carried  
113 out under operative conditions could be complementary to batch tests as an operational tool.

## 114 **2. Material and methods**

### 115 *2.1. $\mu$ GACs*

116 The seven  $\mu$ GACs were activated or reactivated by steam. Three  $\mu$ GACs were regenerated: ReSorb MC (RS,  
117 Jacobi) regenerated from AquaSorb 630 (AS-6, from aggregated mineral base, Jacobi), Norit REACT 2442  
118 (NR, Cabot) regenerated from Norit GAC 2442 (NG, from re-aggregated coal, Cabot) and CycleCarb 305  
119 (CC, from bituminous coal, Calgon Carbon) also produced from a regenerated AC. The other  $\mu$ GACs studied  
120 were PC 1000 300 (PC, from vegetal material, DaCarb) and AquaSorb 2000 (AS-2, from bituminous coal,  
121 Jacobi).  $\mu$ GACs were dried for 24 h at 105 °C prior to each experiment.

### 122 *2.2. $\mu$ GACs chemical, physical and textural characterization*

123 The physical, textural and chemical properties commonly described in the literature for AC and determined in  
124 this study are listed in Table S1 along with the method used and the theory or model applied for calculations.

125 Nitrogen at 77.4 K adsorption – desorption isotherms were obtained to examine textural properties. Tube tests  
126 measurements and helium pycnometry were performed to determine the apparent density and the density,  
127 respectively. Elemental analysis was performed to evaluate the carbon, hydrogen, nitrogen, sulfur, oxygen and  
128 ash contents. Mass titration was used to measure  $\text{pH}_{\text{pzc}}$ , and Boehm titration allowed the quantification of total  
129 basic and total acidic groups. SEM-EDX analyses were performed to determine the mineral impurities on  
130  $\mu\text{GACs}$  surface. The particle size distribution was determined using a sieve shaker (AS 200 digit, Retsch) with  
131 8 sieves (800, 630, 500, 400, 315, 160, 100 and  $< 100 \mu\text{m}$ ). 100 g of  $\mu\text{GAC}$  sample were shaken for 10 min  
132 and the mass retained by each sieve was weighed and the intercept for 50% of the cumulative mass ( $d_{50}$ ) was  
133 calculated. More information about the methods and experimental details are available in the supplementary  
134 information (Text S1).

135 The methylene blue number, defined as the amount of methylene blue (MB) adsorbed on a porous material, is  
136 a common indicator to evaluate the adsorptive capacity of an AC for OMPs with a close molecular size  
137 (Lussier et al., 1994; Raposo et al., 2009). 0.5 L of 400 mg/L MB solution (VWR) was placed in a beaker with  
138 0.625 g of activated carbon at room temperature and under controlled stirring on a jar test bench. The  
139 experiment was stopped when the adsorption equilibrium was reached for each  $\mu\text{GAC}$  ( $\text{UV}_{254}$  removal  
140 variation  $< 1\%$ ) and the samples were then filtered on a  $0.45 \mu\text{m}$  PVDF filter before analysis. A second  
141 experiment was conducted with similar operational conditions and the same particle size for all  $\mu\text{GACs}$   
142 (crushed and sieved between 50 and  $63 \mu\text{m}$ ) to overcome the influence of particle size and evaluate the effect  
143 of other characteristics. The contact time was reduced to 30 min (similar contact time to batch tests performed  
144 with OMPs) since adsorption kinetics are much faster for PAC than for  $\mu\text{GAC}$ . Residual MB concentrations  
145 were determined with UV absorbance at 254 nm (Genesys 10S UV-VIS spectrophotometer, Thermo  
146 Scientific) based on a calibration range (0-400 mg/L).

### 147 *2.3. Batch tests*

148 Prior to the batch tests,  $\mu\text{GACs}$  were crushed and sieved between 50 and  $63 \mu\text{m}$  to ensure proper adsorption  
149 after 30 min and to avoid the influence of particle size which would have masked the influence of other  
150 properties. Nitrified water (secondary wastewater effluent,  $\text{pH} = 7.2$ , temperature =  $19 \text{ }^\circ\text{C}$ ) was sampled before  
151 the denitrification stage from the Seine Centre WWTP (Colombes, France) (Text S2). 1.5 L of the nitrified

152 water was placed in a glass bottle with 15 mg of activated carbon (dose of 10 mg/L) at room temperature and  
153 under strong stirring (300 rotation per minute) on a stirring table during 30 min. At the end of the experiment,  
154 appropriate volumes of samples were homogenized and filtered on 0.7  $\mu\text{m}$  GF/F glass filters (Whatman) prior  
155 to analyses. Multiple tests have shown that for an identical activated carbon dose (10 mg/L, CycleCarb 305)  
156 and a similar water quality, the removal of micropollutants is not very variable ( $< 10\%$ , Figure S1) and  
157 negligible compared to the variability observed here between coals. As a result, experiments with other AC  
158 were carried out only once. Dissolved organic carbon (DOC) was analyzed by the certified SIAAP laboratory  
159 (NF EN 1484, limit of quantification = 0.3 mgC/L). 28 OMPs (21 pharmaceuticals, 6 pesticides and 1  
160 perfluorinated acid) were analyzed within 48 h at the Institute of Analytical Sciences (ISA – Villeurbanne,  
161 France) by liquid chromatography coupled to tandem mass spectroscopy (Vulliet et al., 2011). Information  
162 about OMPs physico-chemical characteristics and the analytical procedures used are provided in the  
163 supporting information (Table S2). OMPs removal was calculated following the approach of Choubert et al.  
164 (2017), which stated that the uncertainty on OMP concentrations in wastewater generally ranges from 30% to  
165 100% when the measured value is lower than 2.5 to 10 times the limit of quantification (LOQ) of the  
166 compound. Therefore, when a compound was quantified at levels above 5 times the LOQ in the nitrified water  
167 and above the LOQ after adsorption, the removal was conventionally calculated. When a compound  
168 concentration was above 5 times the LOQ in the nitrified water but below the LOQ after adsorption, the  
169 removal was estimated using LOQ/2. Removals were not calculated when concentrations in both the nitrified  
170 water and after adsorption ranged between the LOQ and 5 times the LOQ.  $\text{UV}_{254}$  was measured directly after  
171 sampling and filtration on 0.45  $\mu\text{m}$  polyvinylidene fluoride filters (Milex<sup>®</sup>, Merck) in a 1 cm quartz cuvette  
172 using a spectrophotometer (Genesys 10S UV-Vis, Thermo Scientific).

#### 173 *2.4. Column tests*

174 Continuous-flow column tests were performed at the Seine Centre WWTP. The nitrified water was pumped  
175 at a controlled ascending flow (14 L/h) in polyvinyl chloride columns operated in parallel (height = 100 cm,  
176 diameter = 4.2 cm, cross section = 13.8  $\text{cm}^2$ , volume = 1380  $\text{cm}^3$ ) (Figure S2). 115 g of  $\mu\text{GAC}$  were introduced  
177 to get the same mass per volume of water as in the large-scale pilot studied in previous researches (83.7  $\text{kg}/\text{m}^3$ ,  
178 CarboPlus<sup>®</sup>, Saur) (Mailler et al., 2016a). The fluidized carbon bed height was measured for various ascending  
179 water velocities (ranging from 0 to 20 m/h) to determine  $\mu\text{GACs}$  bed expansion. Due to excessive expansion



180 in the case of PC  $\mu$ GAC, the ascending water velocity was limited to 10 m/h to avoid carbon mass loss. The  
181 results reported in literature show that UV<sub>254</sub> removal can provide a good estimation of organic matter  
182 adsorption and can be used to monitor OMPs removal (Altmann et al., 2016; Mailler et al., 2016a;  
183 Zietzschmann et al., 2014; Ziska et al., 2016). Therefore, the adsorption performances of the 7  $\mu$ GACs under  
184 operative conditions close to those of a full-scale application were evaluated by measuring UV<sub>254</sub> at the  
185 entrance and at the exit of the columns. UV<sub>254</sub> was first measured every hour (0-8h) then twice a day until the  
186 bed equilibrium was reached (UV<sub>254</sub> removal variation < 1%).

## 187 2.5. Statistical analysis

188 Data were treated with the R software (R Core Team, 2007) with the *Hmisc* package (E Harrel Jr, 2017) and  
189 the *rcorr* function in order to explore for possible correlations between  $\mu$ GACs properties, OMPs removal and  
190 column tests results.

## 191 3. Results

### 192 3.1. $\mu$ GACs characterization

#### 193 3.1.1. $\mu$ GACs physical, textural and chemical properties

194 The properties of the 7  $\mu$ GACs are summarized in Table 1. The values obtained for the BET surface were  
195 lower for CC, RS and NR (748, 527 and 885 m<sup>2</sup>/g, respectively) which are regenerated  $\mu$ GACs, showing as  
196 expected that reactivation had a substantial negative impact on ACs textural properties (Han et al., 2014). The  
197 BET surface was positively correlated with both the total porous volume ( $r_{\text{Pearson}} = 0.85$ , p-value = 0.014), the  
198 microporous volume ( $r_{\text{Pearson}} = 0.99$ , p-value < 0.001), the percentage of microporous volume ( $r_{\text{Pearson}} = 0.96$ ,  
199 p-value < 0.001) and negatively correlated with the average pore size ( $r_{\text{Pearson}} = -0.95$ , p-value = 0.001). As  
200 expected, the decrease of the average pore size induces the increase of both the BET surface and the  
201 microporous volume value and percentage. As indicated by the shape of the hysteresis loops from nitrogen  
202 adsorption-desorption isotherms (Figure S3), these micro-mesoporous carbons (i.e. microporous +  
203 mesoporous volume > 75%) exhibited different pore volume distributions. The microporous, mesoporous and  
204 macroporous volumes were similarly distributed for CC, AS-2, NG and NR. On the contrary, PC and AS-2

205 exhibited a higher microporous and macroporous volume but a lower mesoporous volume. Finally, RS  
206 exhibited the lowest microporous volume and the highest macroporous volume.

207 The ash content ranged from 4.4 to 18.5% and its variation among  $\mu$ GACs may be due to differences in the  
208 nature of the raw materials used, as well as for mineral impurities on  $\mu$ GACs surface (Table S3). The  $\text{pH}_{\text{pzc}}$   
209 for the studied  $\mu$ GACs ranged from 8.4 to 11.2. Consequently, the surface of the  $\mu$ GACs should be globally  
210 positively charged at the pH of conventional WWTP effluents (i.e.  $\text{pH} \sim 7$  to 8) and electrostatic interactions  
211 are thus expected between  $\mu$ GACs surface, OMPs and DOM, the latter one being negatively charged in those  
212 pH conditions (Margot et al., 2013; Yu et al., 2012). According to the measured  $\text{pH}_{\text{pzc}}$  values,  $\mu$ GACs exhibited  
213 higher concentrations of basic groups than acidic groups (except for AS-2). The  $\text{pH}_{\text{pzc}}$  values of  $\mu$ GACs were  
214 positively correlated with their basic group concentrations ( $r_{\text{Pearson}} = 0.81$ ,  $p\text{-value} = 0.027$ ) and negatively  
215 correlated with their acidic group concentrations ( $r_{\text{Pearson}} = -0.84$ ,  $p\text{-value} = 0.018$ ).

216  $\mu$ GACs apparent density was in the range 0.43-0.47  $\text{g}/\text{cm}^3$  (except for AS-2 with 0.53  $\text{g}/\text{cm}^3$ ), close to a value  
217 reported for a widely used GAC (FiltruSorb 400, 0.43  $\text{g}/\text{cm}^3$ , Al-Degs et al. (2000)), and their density was in  
218 the range 2.19-2.33  $\text{g}/\text{cm}^3$ . Sieving showed that the studied  $\mu$ GACs have a particle size distribution ranging  
219 from 250 to 600  $\mu\text{m}$  except PC (100 to 400  $\mu\text{m}$ ) and AS-2 (500 to > 800  $\mu\text{m}$ ) (Figure S4).

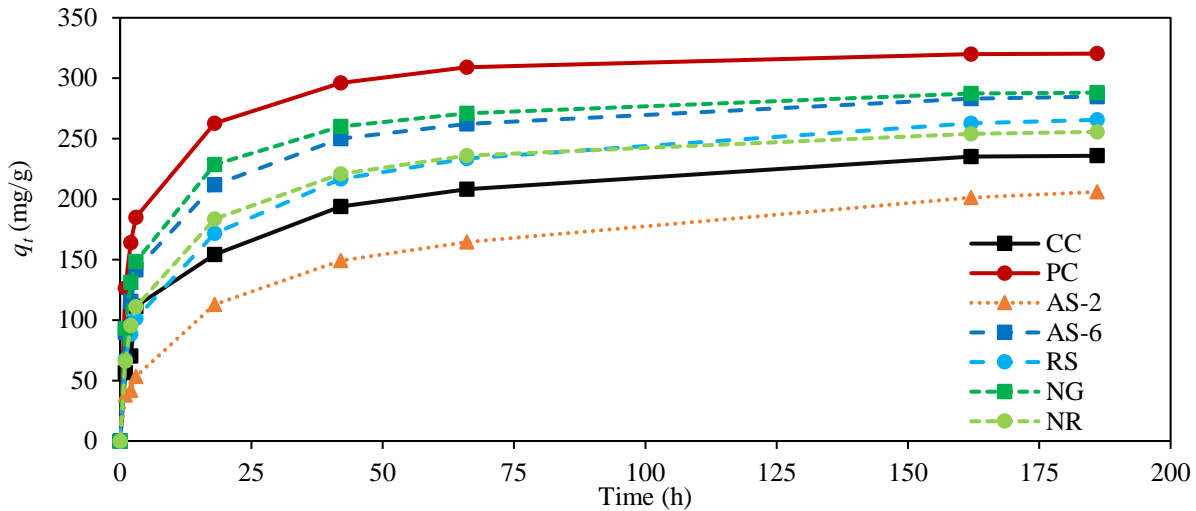
### 220 3.1.2. Methylene blue number

221 MB adsorption was fast until 18 h, then slowed down and reached equilibrium after 160 h with final values  
222 (i.e. MB numbers) ranging from 200 to 320  $\text{mg}/\text{g}$  (Figure 1), similar to those obtained at  $\text{pH} = 5.0$  after 160 h  
223 from commercial GACs prepared with similar raw material (Wang et al., 2005) or with different raw materials  
224 (Rafatullah et al., 2010), and from non-commercial GACs after 48 h (Raposo et al., 2009). The MB number  
225 was negatively correlated with the particle size ( $d_{50}$ ,  $r_{\text{Pearson}} = 0.93$ ,  $p\text{-value} = 0.003$ ), confirming that MB and  
226 by extension OMPs adsorption kinetics are controlled by particle size (Delgado et al., 2012; Raposo et al.,  
227 2009; Shi et al., 2014). The MB number was also negatively correlated with the ash content ( $r_{\text{Pearson}} = -0.77$ ,  
228  $p\text{-value} = 0.041$ ). Similar observations were reported for the adsorption of bisphenol A which was more  
229 important when the mineral content decreased (Bautista-Toledo et al., 2005). According to the authors, the  
230 decrease of the mineral content increased the hydrophobicity of the AC which increased the adsorption of  
231 bisphenol A.

232 Table 1. Properties of the seven  $\mu$ GACs. CC = CycleCarb 305, PC = PC 1000 300, AS-2 = AquaSorb 2000, AS-6 =  
 233 AquaSorb 630, RS = ReSorb MC, NG = Norit GAC 2442 and NR = Norit REACT 2442. \*: MB adsorption after 30 min  
 234 and an identical particle size for all  $\mu$ GACs (50-63  $\mu$ m).

Properties	Micro-grain activated carbon						
	CC	PC	AS-2	AS-6	RS	NG	NR
BET surface (m <sup>2</sup> /g)	748	1255	1006	954	527	1012	885
Total porous volume (cm <sup>3</sup> /g)	0.33	0.38	0.32	0.37	0.25	0.35	0.33
Microporous volume (cm <sup>3</sup> /g)	0.18	0.29	0.24	0.23	0.12	0.25	0.22
Mesoporous volume (cm <sup>3</sup> /g)	0.15	0.05	0.03	0.11	0.08	0.09	0.11
Macroporous volume (cm <sup>3</sup> /g)	< 0.01	0.03	0.05	0.03	0.06	0.02	< 0.01
Microporous volume (%)	53	79	73	61	46	69	66
Mesoporous volume (%)	46	12	10	30	31	25	34
Macroporous volume (%)	1	9	17	9	23	6	0
Average pore size (nm)	2.8	1.9	2.0	2.4	3.0	2.2	2.3
Average micropore size (nm)	0.8	0.8	0.9	0.8	0.8	0.8	0.8
Average mesopore size (nm)	6.7	6.6	6.6	8.1	6.9	8.1	7.2
Ash content (%)	18.5	4.4	16.2	13.5	12.4	12.0	9.2
C content (%)	78.6	91.4	82.0	84.8	83.3	85.5	88.5
H content (%)	0.3	0.5	0.4	0.5	0.5	0.3	0.4
N content (%)	0.3	0.4	0.4	0.3	0.5	0.4	0.4
S content (%)	1.2	0.1	0.6	0.1	0.4	0.5	0.4
O content (%)	1.1	3.2	0.4	0.8	3.0	1.3	1.1
pH <sub>pzc</sub>	10.9	9.8	9.3	10.5	11.2	8.4	9.4
Basic groups ( $\mu$ mol/g)	512	436	66	400	558	236	209
Acid groups ( $\mu$ mol/g)	62	88	71	45	59	156	96
d <sub>50</sub> ( $\mu$ m)	517	198	689	362	357	439	439
Apparent density (g/cm <sup>3</sup> )	0.47	0.44	0.53	0.43	0.46	0.45	0.47
Density (g/cm <sup>3</sup> )	2.27	2.31	2.25	2.25	2.19	2.33	2.30
MB number (mg/g)	234	320	206	285	266	288	254
MB adsorption* (mg/g)	126	225	157	151	155	194	164

235 A second experiment was performed in the same operational conditions but using a similar particle size for all  
 236  $\mu$ GACs (crushed and sieved between 50 and 63  $\mu$ m) to overcome the influence of the particle size. MB  
 237 adsorption after 30 min was negatively correlated with the ash content ( $r_{\text{Pearson}} = -0.86$ , p-value = 0.013) but  
 238 positively correlated with the carbon content ( $r_{\text{Pearson}} = 0.85$ , p-value = 0.017). Those results confirmed that the  
 239 presence of mineral elements impaired MB adsorption. MB adsorption was correlated to a lesser extent with  
 240 the BET surface ( $r_{\text{Pearson}} = 0.73$ , p-value = 0.063) which indicates that MB adsorption can only be used to  
 241 compare the adsorption capacity of AC with a similar particle size.



243

244 Figure 1. Evolution of the quantity of MB adsorbed ( $q_t$ , mg of methylene blue per g of  $\mu$ GAC) on the seven  $\mu$ GACs in  
 245 batch tests during 186 h (initial MB concentration = 400 mg/L, activated carbon concentration = 0.625 g/L).

### 246 3.1.3. Expansion test

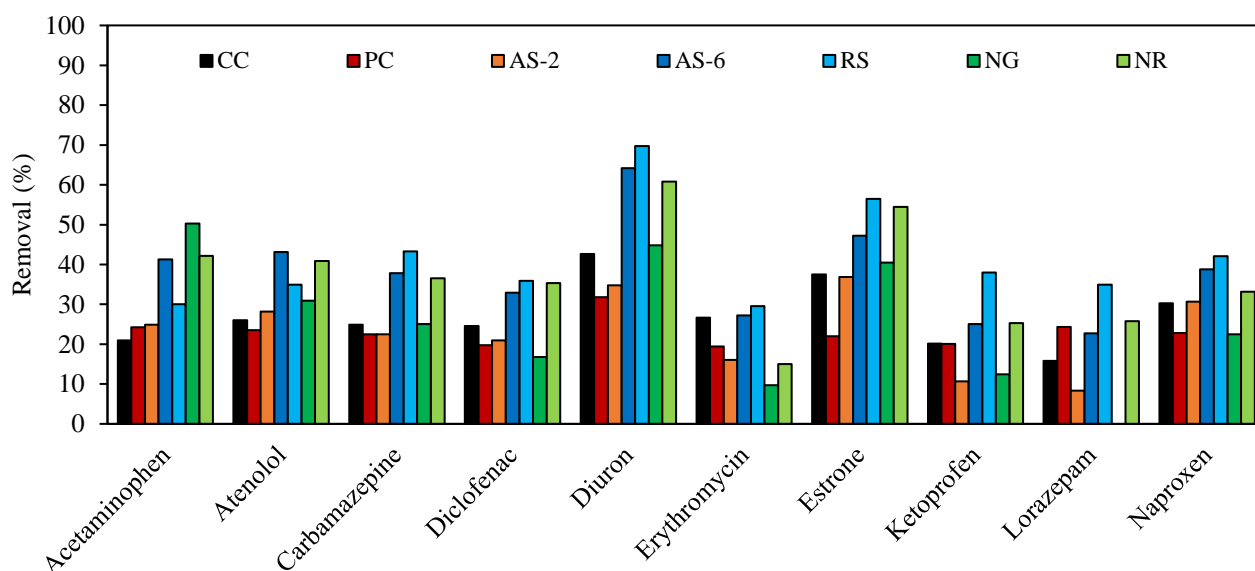
247 Bed expansion was measured in continuous-flow column experiments to determine the behavior of each  
 248  $\mu$ GAC in conditions similar to those applied to a full-scale CarboPlus<sup>®</sup> process (i.e. continuous flow with up  
 249 to 15 m/h fluid velocity). Bed expansion started to increase linearly above a fluid velocity of 4-6 m/h, except  
 250 for PC (2 m/h) and AS-2 (10 m/h) (Figure S5), and it was negatively correlated with the particle size ( $d_{50}$ ,  
 251  $r_{\text{Pearson}} = -0.97$ ,  $p$ -value < 0.001) as expected from the Ergun equation which is used for describing fluidized  
 252 bed expansion (Ergun and Orning, 1949). The particles density can also exert an influence on expansion, with  
 253 dense particles requiring high up-flow velocity to achieve expansion (Bello et al., 2017). However, the density  
 254 was not the main parameter controlling bed expansion in our experiments because all  $\mu$ GACs had similar  
 255 density. AS-2 exhibited a limited expansion (i.e. bed expansion of only ~ 10-20% at 15 m/h), which would  
 256 lead to insufficient particle mixing, heat and mass transfers in a reactor at the industrial scale and therefore to  
 257 reduced adsorption performances (Bello et al., 2017). On the other hand, PC exhibited excessive expansion  
 258 leading to mass loss at fluid velocities higher than 10 m/h, which would be detrimental for a use at the pilot  
 259 scale (e.g. in the CarboPlus<sup>®</sup> process).

### 260 3.2. OMPs adsorption test

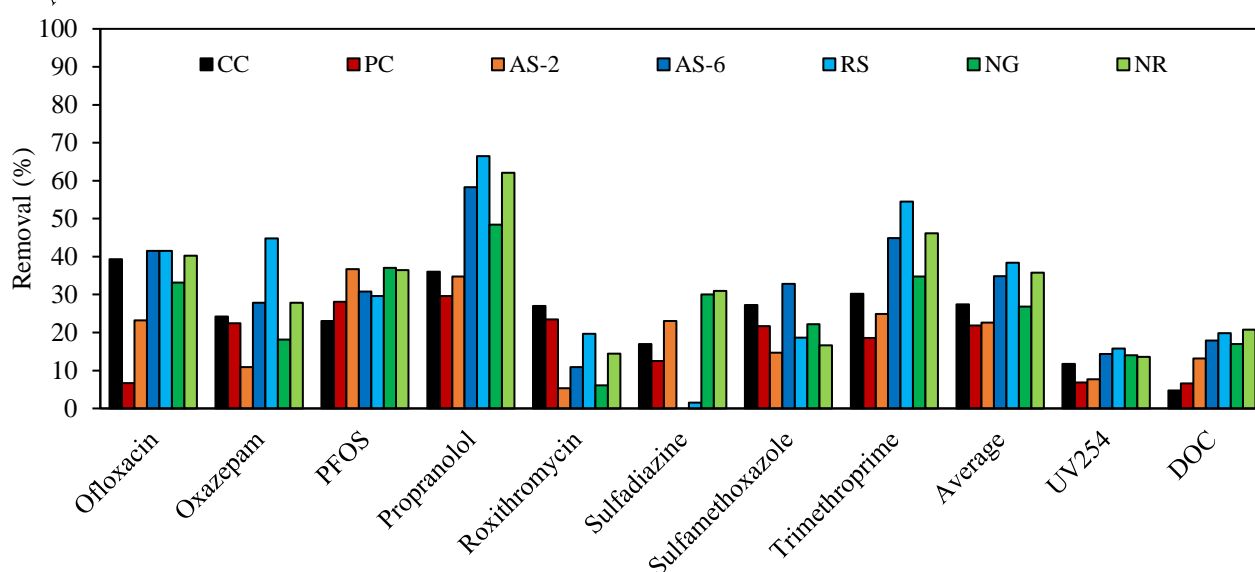
261 Out of the 28 OMP monitored, 7 OMPs (acetamiprid, clothianidin, estrone, ibuprofen, imidacloprid,  
 262 thiacloprid and thiamethoxam) were not detected in the secondary wastewater effluent. The OMPs

263 concentration ranged from 8 ng/L for PFOS to 805 ng/L for sulfamethoxazole (Table S2). Ciprofloxacin,  
264 norfloxacin and tetracycline were quantified in the wastewater but their removal was not calculated (values  
265 close to their respective LOQ). The OMPs, UV<sub>254</sub>, DOC removals and average OMPs removal for each  $\mu$ GAG  
266 are illustrated in Figure 2.

267 Among the 18 OMPs considered, the highest OMPs removals were obtained for RS (average removal  $\pm$   
268 standard deviation =  $38 \pm 16\%$ ), NR ( $34 \pm 16\%$ ), AS-6 ( $35 \pm 15\%$ ) followed by CC ( $27 \pm 7\%$ ) and NG ( $27 \pm$   
269  $14\%$ ), while the lowest average removals were obtained for PC ( $22 \pm 6\%$ ) and AS-2 ( $23 \pm 10\%$ ) (Figure 2).  
270 These results could be surprising since PC showed the highest values of BET surface ( $1\,255\text{ m}^2/\text{g}$ ), total porous  
271 volume ( $0.376\text{ cm}^3/\text{g}$ ) and microporous volume ( $0.295\text{ cm}^3/\text{g}$ ), while RS had the lowest values of BET surface  
272 ( $527\text{ m}^2/\text{g}$ ), total porous volume ( $0.252\text{ cm}^3/\text{g}$ ) and microporous volume ( $0.117\text{ cm}^3/\text{g}$ ). There was actually a  
273 negative correlation between the average OMPs removal and the BET surface ( $r_{\text{Spearman}} = -0.79$ , p-value =  
274  $0.033$ ), as well as with the microporous volume ( $r_{\text{Spearman}} = -0.79$ , p-value =  $0.033$ ) and the percentage of  
275 microporous volume ( $r_{\text{Spearman}} = -0.81$ , p-value =  $0.027$ , Figure 3). As previously mentioned (part 3.1.1.), these  
276 4 properties are all linked, which means that the correlations observed with the average removal may reflect a  
277 single phenomenon. The average removal decreased for  $\mu$ GACs with microporous volumes above 65%  
278 (Figure 3), despite the fact that OMPs are generally considered to be preferentially adsorbed into micropores  
279 unlike DOM (Li et al., 2002; Quinlivan et al., 2005). An increase in the percentage of microporous volume  
280 leads to a decrease in macro- and mesoporous volumes, which play a key role in OMPs removal by adsorbing  
281 the DOM also present in the bulk water (Newcombe et al., 2002a). Therefore, for the same amount of DOM  
282 adsorbed, the surface coverage of DOM on AC is globally lower with an increase in the percentage of the  
283 microporous volume but is higher in macro- and mesopores (Li et al., 2003). An increase of the AC surface  
284 coverage by DOM in macro- and mesopores was demonstrated to exert a negative impact on OMPs surface  
285 diffusion, and the pore blockage it caused was higher for AC showing a higher percentage of micropores (Li  
286 et al., 2003).



287



288

289

290

291

Figure 2. OMPs, UV<sub>254</sub>, DOC removals and average OMPs removal for the 7  $\mu$ GACs studied (10 mg/L, crushed and sieved at 50-63  $\mu$ m, initial UV<sub>254</sub> = 0.204 1/cm and initial DOC = 10.6 mgC/L) after 30 min of contact time with nitrified water.

292

293

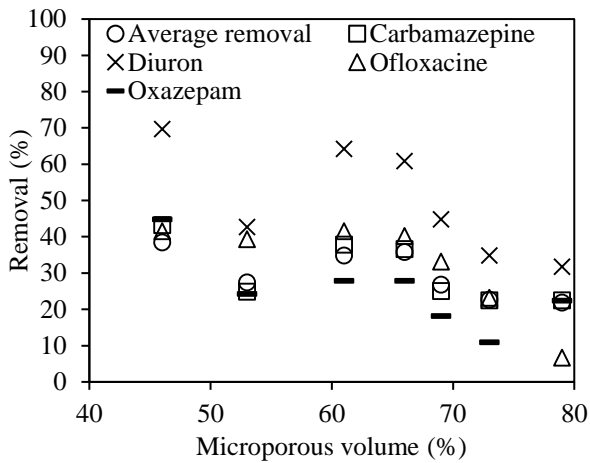
294

295

296

297

A positive correlation was observed between the average removal and the average pore size ( $r_{\text{Spearman}} = 0.81$ ,  $p\text{-value} = 0.027$ ), but no correlation was found with MB adsorption for a similar particle size. Several molecules (carbamazepine, diuron, ofloxacin and oxazepam) exhibited a negative correlation between their removal and the percentage of micropores ( $r_{\text{Spearman}} = -0.78$ ,  $-0.79$ ,  $-0.87$  and  $-0.78$  and  $p\text{-value} < 0.05$ , respectively) (Figure 3). The percentage of microporous volume should not exceed 65 % to ensure DOM adsorption in macro- and mesopores and to avoid micropores blockage.



298

299

300 Figure 3. Removal of selected OMPs and the average removal of the 18 OMPs according to the percentage of microporous  
 301 volume for the 7  $\mu$ GACs studied (10 mg/L, crushed and sieved at 50-63  $\mu$ m) after 30 min of contact time with nitrified  
 302 water.

303  $\mu$ GACs surface chemistry also had an impact on OMPs adsorption. A positive correlation was observed

304 between the  $\text{pH}_{\text{pzc}}$  and the removal of erythromycin ( $r_{\text{Spearman}} = 0.93$ ,  $p\text{-value} = 0.007$ ) while a negative

305 correlation was found for PFOS ( $r_{\text{Spearman}} = -0.82$ ,  $p\text{-value} = 0.034$ ). The increase of the point of zero charge,

306 thus the positive charges on the activated carbon surface, improved the adsorption of the DOM which was

307 negatively charged at the pH of the effluent. Moreover, DOM adsorption can modify the net charge of the

308 activated carbon surface to negative values and consequently increase the adsorption of erythromycin

309 (positively charged) and decrease the adsorption of PFOS (negatively charged). In the same way, a positive

310 correlation was also found between the quantity of basic groups and roxithromycin ( $r_{\text{Spearman}} = -0.79$ ,  $p\text{-value}$

311  $= 0.048$ ) which is positively charged, while a positive correlation was observed between the quantity of acidic

312 groups and sulfadiazine ( $r_{\text{Spearman}} = -0.86$ ,  $p\text{-value} = 0.024$ ) which is mostly negatively charged. The absence

313 of correlation for other positively (atenolol, propranolol and trimethoprim) and negatively charged compounds

314 (diclofenac, ketoprofen, naproxen, ofloxacin and sulfamethoxazole) indicated that other phenomena

315 influenced their adsorption. These phenomena could include hydrophobic interactions and hydrogen bonds.

316 The study of these interactions, whom study requires specific experiments (e.g. modification of activated

317 carbon surface chemistry, Mahajan et al., 1980) or analytical techniques (e.g. FTIR, Tran et al., 2017a), is

318 more complex than that of electrostatic interactions, and the presence of dissolved organic matter also

319 complicates the interpretations.

320 The mineral composition of the nitrified water was not determined during the study (except nitrogenous and

321 phosphorous species), but the concentrations of most minerals were available for the WWTP treated water

322 and are presented in Table S4. The chemical composition (in terms of nutrients) of the nitrified is also available  
323 in the supplementary material (Table S5). Inorganic ions could influence the electrostatic interactions between  
324 activated carbon, dissolved organic matter and micropollutants as observed at the surface of membranes used  
325 in filtration processes. The formation of cation bridges was indeed reported between the membrane surface  
326 and DOM in the presence of calcium ions (Bellona et al., 2004). The confirmation of such an impact of  
327 inorganic species on the adsorption of OMPs and DOM would require additional experiments.

328 No correlation was found between any specific OMPs property and the removal on each  $\mu$ GAC. Adsorption  
329 is a complex process resulting from the influence of several OMPs properties such as the charge, the size, the  
330 hydrophobicity or the presence of specific groups. The obtained removals can be explained by analyzing the  
331 physico-chemical properties of each targeted compound and their link with  $\mu$ GACs characteristics. For some  
332 OMPs, limiting and/or strongly drifting factors can be highlighted. Erythromycin and roxithromycin are large  
333 compounds (molar mass > 700 g/mol) with a minimal projection area of 55 and 69  $\text{\AA}^2$ , respectively. The  
334 average micropore size of most  $\mu$ GACs was 8  $\text{\AA}$ , which gave an opening area of 50  $\text{\AA}^2$  based on the assumption  
335 that micropores are cylindrical. These two OMPs were therefore too large to access most micropores, which  
336 explained their reduced adsorption capacity and thus their low removal (i.e. the average removal for the 7  
337  $\mu$ GACs was 21% for erythromycin and 15% for roxithromycin). Moreover, they may have been subject to  
338 steric hindrance with the DOM during diffusion from the water to the activated carbon pores, as well as  
339 competition for adsorption sites on larger micropores and mesopores.

340 The positively charged compounds atenolol, propranolol and trimethoprim were among the best removed  
341 OMPs (average removal for the 7  $\mu$ GACs of 33, 48 and 36%, respectively). However, no correlation was  
342 observed between their removal and  $\text{pH}_{\text{pzc}}$  values. This difference from other OMPs was attributed to the  
343 presence of DOM, which modified the surface chemistry and thus inhibited the effect of the  $\text{pH}_{\text{pzc}}$  of  $\mu$ GACs  
344 (Newcombe, 1994; Yu et al., 2012). Adsorption of the positively charged compounds was therefore favored  
345 by attractive electrostatic interactions with the negatively charged DOM adsorbed onto the activated carbon.  
346 Propranolol exhibited the highest removal, probably because its minimal projection area was lower (32  $\text{\AA}^2$   
347 compared to 42  $\text{\AA}^2$  for atenolol and 38  $\text{\AA}^2$  for trimethoprim), thus it was less subjected to steric hindrance with  
348 DOM and could access to smaller micropores.



349 The negatively charged compounds diclofenac, ketoprofen, sulfadiazine and sulfamethoxazole were less  
350 removed than other OMPs (average removal between the 7  $\mu$ GACs ranging from 16 to 27%). This can be  
351 explained by the repulsive electrostatic interactions existing with the negatively charged DOM adsorbed onto  
352 the activated carbon surface. However, other negatively charged compounds (naproxen, ofloxacin and PFOS)  
353 were better removed (31-32%), which suggests that other properties played a role in their adsorption.  
354 Naproxen and ofloxacin have linked aromatic rings which may have created  $\pi$ - $\pi$  interactions with  $\mu$ GACs  
355 aromatic rings. PFOS is a fluorosurfactant with a hydrophilic sulfonate group and a hydrophobic fluorinated  
356 chain which may have favored its presence at the water/solid interface and thus its adsorption.

357 Various removals were obtained for neutral compounds: an important adsorption was observed for diuron and  
358 estrone (average removals for the 7  $\mu$ GACs were 50 and 42%, respectively), a medium adsorption for  
359 acetaminophen and carbamazepine (average removals of 33 and 30%, respectively) and a low removal for  
360 lorazepam and oxazepam (average removal of 19 and 25%, respectively). Carbamazepine, lorazepam and  
361 oxazepam (minimal projection area  $> 33 \text{ \AA}^2$ ) are larger than acetaminophen, diuron and estrone ( $< 28 \text{ \AA}^2$ ) and  
362 thus were probably subjected to a higher steric hindrance with DOM and could access to smaller micropores.  
363 Acetaminophen was less adsorbed and is less hydrophobic ( $\log D = 0.91$  at pH 8) than diuron and estrone ( $\log$   
364  $D = 2.53$  and  $4.31$  at pH 8, respectively), which suggests that the hydrophobicity could also play a role for the  
365 adsorption of neutral compounds.

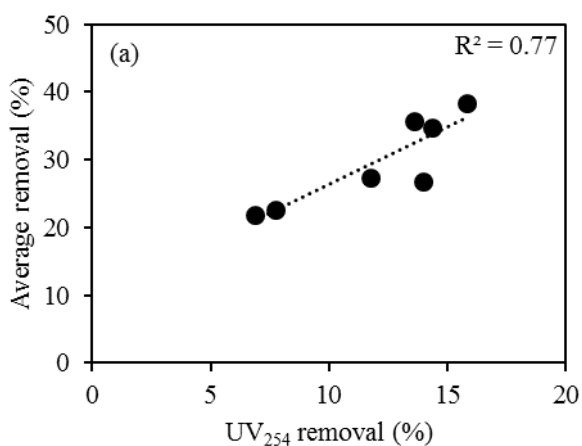
### 366 3.3. *UV<sub>254</sub> and DOC removal*

#### 367 3.3.1. Batch tests

368  $UV_{254}$  (initial value = 0.204 mgC/L) and DOC (initial value = 10.6 mgC/L) were measured in the batch  
369 experiments to study the adsorption of DOM in conjunction with OMPs. The highest  $UV_{254}$  removals were  
370 obtained for AS-6, RS, NG and NR (14-15%), then CC (12%) and last PC and AS-2 (7-8%). The  $UV_{254}$   
371 removal was negatively correlated with the percentage of microporous volume ( $r_{\text{Pearson}} = -0.75$ , p-value =  
372 0.052), which confirmed that a higher proportion of both meso- and macroporous volumes favored the  
373 adsorption of DOM. AS-6, RS, NG and NR were also the most efficient at removing DOC (17-21%), followed  
374 by AS-2 (13%), CC (5%) and PC (7%).

375 There was a strong positive correlation between the  $UV_{254}$  removal and the OMPs average removal ( $r_{\text{Pearson}} =$   
376 0.88, p-value = 0.010), carbamazepine ( $r_{\text{Pearson}} = 0.80$ , p-value = 0.032), diuron ( $r_{\text{Pearson}} = 0.89$ , p-value = 0.008),  
377 estrone ( $r_{\text{Pearson}} = 0.88$ , p-value = 0.010), ofloxacin ( $r_{\text{Pearson}} = 0.90$ , p-value = 0.006), propranolol ( $r_{\text{Pearson}} =$   
378 0.90, p-value = 0.006) and trimethoprim ( $r_{\text{Pearson}} = 0.93$ , p-value = 0.003) (Figure 4). Those molecules were  
379 among the most removed, which suggested that  $UV_{254}$  could only be used to predict the removal of OMPs that  
380 were well adsorbed. Correlations were also obtained between the DOC removal and the average OMPs  
381 removal ( $r_{\text{Pearson}} = 0.76$ , p-value = 0.046) (Figure 4), atenolol ( $r_{\text{Pearson}} = 0.83$ , p-value = 0.020), diuron ( $r_{\text{Pearson}} =$   
382 0.77, p-value = 0.046), estrone ( $r_{\text{Pearson}} = 0.020$ , p-value = 0.83), propranolol ( $r_{\text{Pearson}} = 0.89$ , p-value = 0.007)  
383 and trimethoprim ( $r_{\text{Pearson}} = 0.81$ , p-value = 0.027).

384 These correlations suggested that DOM and OMPs followed similar adsorption mechanisms onto activated  
385 carbon or that they interacted (e.g. electrostatic interactions) and were adsorbed together as suggested by  
386 several studies (Aristilde and Sposito, 2013; Aschermann et al., 2019; Liu et al., 2014). Correlations between  
387 OMPs removal and  $UV_{254}$  were also observed in other studies (Anumol et al., 2015; Mailler et al., 2016a;  
388 Zietzschmann et al., 2014), which confirmed the relevance of  $UV_{254}$  as a surrogate for the monitoring of  
389  $\mu\text{GACs}$  performances regarding OMPs adsorption.



390

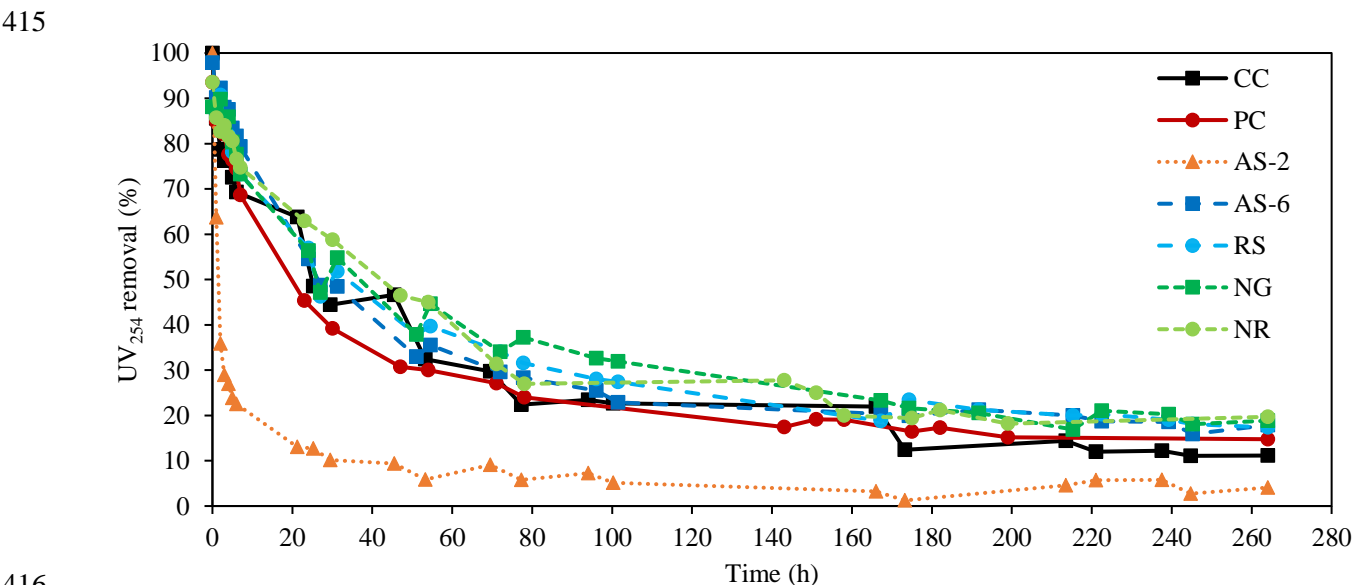
391 Figure 4. Average OMPs removal (%) versus  $UV_{254}$  removal (%) after 30 min of contact with nitrified water (10 mg/L of  
392 activated carbon, crushed and sieved at 50-63  $\mu\text{m}$ , initial value for  $UV_{254} = 0.204$  1/cm).

393 3.3.2. Column tests

394  $UV_{254}$  removal was investigated in continuous-flow column tests in order to compare the performances of  
395  $\mu\text{GACs}$  between batch experiments and operative conditions closer to full-scale application, and to obtain

396 supplementary information on the influence of  $\mu$ GACs properties on  $UV_{254}$  removal. For each  $\mu$ GAC, the  
 397  $UV_{254}$  removal decreased rapidly during the first 20 hours and stabilized after 200 hours between 10 and 20%  
 398 except for AS-2 (4%) for which it started to stabilize after only 7 hours (Figure 5). This plateau indicated that  
 399 adsorption still took place in the columns even if the system reached the equilibrium. It could be due to slow  
 400 diffusion in pores or to the development of a biological activity on  $\mu$ GACs which degraded the adsorbed DOM  
 401 and thus liberated some pores for further adsorption. At the end of the experiment, the  $UV_{254}$  removal was the  
 402 highest for AS-6, RS, NG and NR (17-20%), then PC (15%), CC (11%) and last AS-2 (4%). This classification  
 403 of  $\mu$ GACs is different from batch tests where the highest  $UV_{254}$  removals were obtained for AS-6, RS, NG  
 404 and NR, then CC and last PC and AS-2. No correlations were found with  $\mu$ GACs characteristics.

405 The low performances of AS-2 were attributed to its limited expansion which reduced the mass transfer from  
 406 the effluent to the AC surface. Its high percentage of micropores may have also impaired DOM adsorption.  
 407 Despite higher expansion, surface area and total volume, PC exhibited a  $UV_{254}$  removal similar to those  
 408 obtained with other  $\mu$ GACs. This could be due to its relatively high ratio microporous volume/mesoporous  
 409 volume which limited its ability to adsorb all DOM fractions and thus increased competition between OMPs  
 410 and DOM and the pore blockage effect. In contrast to AS-2, the smaller particles size of PC allowed it to  
 411 compensate the negative impact of its high percentage of microporous volume by a higher expansion and  
 412 probably faster adsorption kinetics. The particles size is, as expected, an important characteristic to be  
 413 considered when selecting an activated carbon for an industrial application in the case of a process in fluidized  
 414 bed.



417 Figure 5. UV<sub>254</sub> breakthrough curves for the seven  $\mu$ GACs in continuous-flow columns (115 g per column) with nitrified  
418 water (233 mL/min) for 11 days.

#### 419 **4. Conclusions**

420 The physical, textural and chemical characterization of the 7  $\mu$ GACs and the batch tests performed with  
421 secondary wastewater effluent revealed the influence of several  $\mu$ GACs properties on OMPs adsorption. An  
422 increase in the percentage of microporous volume leads to a decrease in the percentages of macro- and  
423 mesoporous volumes which play a key role in OMPs removal by adsorbing DOM and thus reducing  
424 micropores blockage. As a recommendation, the percentage of microporous volume should not be higher than  
425 65 % to ensure DOM adsorption in macro- and mesopores and hence to limit micropores blockage. The  
426 adsorption of DOM onto  $\mu$ GACs modified their surface charge from positive to negative. This modification  
427 promoted the adsorption of positively charged OMPs in contrast to negatively charged OMPs.

428 In agreement with the literature, OMPs adsorption did not depend on a single specific OMPs property and  
429 their removal could rather be explained by a combination of their properties. The minimal projection area was  
430 a key property that conditioned the access of OMPs into micropores and influenced their diffusion into  $\mu$ GACs  
431 due to steric hindrance and pore blockage with the adsorbed DOM. As a result, the largest molecules (i.e.  
432 erythromycin and roxithromycin) were subject to size exclusion and exhibited low removals. The highest  
433 removals were obtained with the neutral compounds that showed the highest hydrophobicity values (i.e. log  
434 D). Charge was then another parameter influencing OMPs adsorption through electrostatic interactions with  
435 DOM, positively charged OMPs being more retained on  $\mu$ GACs covered with DOM than negatively charged  
436 OMPs. Other properties (e.g. the presence of hydrophobic functional groups) may explain the various  
437 removals obtained for negatively charged OMPs.

438 A different classification of  $\mu$ GACs for UV<sub>254</sub> removal was obtained between batch tests and column tests  
439 under operative conditions representative of those of a large-scale process. The particle size appeared to be a  
440 key parameter controlling  $\mu$ GACs expansion which had an impact on UV<sub>254</sub> and consequently on OMPs  
441 removal for  $\mu$ GACs. It is therefore recommended, before an application on a full-scale installation, to perform  
442 column tests in order to anticipate these behaviors which cannot be observed in batch.

443 The observed trends between OMPs, UV<sub>254</sub> and DOC removals suggested that DOM and OMPs followed  
444 similar adsorption mechanisms on  $\mu$ GACs or interacted and were adsorbed together. The important role of  
445 DOM in OMPs adsorption and the various mechanisms involved (i.e. pore blockage, co-adsorption) will be  
446 further investigated (e.g. by using fluorescence spectroscopy or size exclusion chromatography) to improve  
447 the understanding of the adsorption process.

## 448 **Acknowledgments**

449 This work was supported by the OPUR research program. The authors would like to thank the SIAAP  
450 laboratory, Céline Briand (SIAAP), Barbara Giroud (ISA), Lila Boudahmane, Martin Maréchal and  
451 Chandirane Partibane (LEESU) for their technical support and their participation to analyses.

## 452 **References**

- 453 Al-Degs, Y., Khraisheh, M.A.M., Allen, S.J., Ahmad, M.N., 2000. Effect of carbon surface chemistry on the  
454 removal of reactive dyes from textile effluent. *Water Res.* 34, 927–935.  
455 [https://doi.org/10.1016/S0043-1354\(99\)00200-6](https://doi.org/10.1016/S0043-1354(99)00200-6)
- 456 Altmann, J., Massa, L., Sperlich, A., Gnirss, R., Jekel, M., 2016. UV<sub>254</sub> absorbance as real-time monitoring  
457 and control parameter for micropollutant removal in advanced wastewater treatment with powdered  
458 activated carbon. *Water Res.* 94, 240–245. <https://doi.org/10.1016/j.watres.2016.03.001>
- 459 Alves, T.C., Cabrera-Codony, A., Barceló, D., Rodriguez-Mozaz, S., Pinheiro, A., Gonzalez-Olmos, R., 2018.  
460 Influencing factors on the removal of pharmaceuticals from water with micro-grain activated carbon.  
461 *Water Res.* <https://doi.org/10.1016/j.watres.2018.07.037>
- 462 Anumol, T., Sgroi, M., Park, M., Roccaro, P., Snyder, S.A., 2015. Predicting trace organic compound  
463 breakthrough in granular activated carbon using fluorescence and UV absorbance as surrogates. *Water*  
464 *Res.* 76, 76–87. <https://doi.org/10.1016/j.watres.2015.02.019>
- 465 Aristilde, L., Sposito, G., 2013. Complexes of the antimicrobial ciprofloxacin with soil, peat, and aquatic  
466 humic substances: Adsorption of ciprofloxacin on humic substances. *Environ. Toxicol. Chem.* n/a-  
467 n/a. <https://doi.org/10.1002/etc.2214>
- 468 Aschermann, G., Neubert, L., Zietzschmann, F., Jekel, M., 2019. Impact of different DOM size fractions on  
469 the desorption of organic micropollutants from activated carbon. *Water Res.* S0043135419304245.  
470 <https://doi.org/10.1016/j.watres.2019.05.039>
- 471 Bello, M.M., Abdul Raman, A.A., Purushothaman, M., 2017. Applications of fluidized bed reactors in  
472 wastewater treatment – A review of the major design and operational parameters. *J. Clean. Prod.* 141,  
473 1492–1514. <https://doi.org/10.1016/j.jclepro.2016.09.148>
- 474 Bellona, C., Drewes, J.E., Xu, P., Amy, G., 2004. Factors affecting the rejection of organic solutes during  
475 NF/RO treatment—a literature review. *Water Res.* 38, 2795–2809.  
476 <https://doi.org/10.1016/j.watres.2004.03.034>
- 477 Benstoem, F., Nahrstedt, A., Boehler, M., Knopp, G., Montag, D., Siegrist, H., Pinnekamp, J., 2017.  
478 Performance of granular activated carbon to remove micropollutants from municipal wastewater—A  
479 meta-analysis of pilot- and large-scale studies. *Chemosphere* 185, 105–118.  
480 <https://doi.org/10.1016/j.chemosphere.2017.06.118>

- 481 Benstoem, F., Pinnekamp, J., 2017. Characteristic numbers of granular activated carbon for the elimination of  
 482 micropollutants from effluents of municipal wastewater treatment plants. *Water Sci. Technol.* 76,  
 483 279–285. <https://doi.org/10.2166/wst.2017.199>
- 484 Bui, X.T., Vo, T.P.T., Ngo, H.H., Guo, W.S., Nguyen, T.T., 2016. Multicriteria assessment of advanced  
 485 treatment technologies for micropollutants removal at large-scale applications. *Sci. Total Environ.*  
 486 563–564, 1050–1067. <https://doi.org/10.1016/j.scitotenv.2016.04.191>
- 487 Choubert, J.-M., Martin Ruel, S., Miege, C., Coquery, M., 2017. Rethinking micropollutant removal  
 488 assessment methods for wastewater treatment plants – how to get more robust data? *Water Sci.*  
 489 *Technol.* 75, 2964–2972. <https://doi.org/10.2166/wst.2017.181>
- 490 Delgado, L.F., Charles, P., Glucina, K., Morlay, C., 2014. Adsorption of Ibuprofen and Atenolol at Trace  
 491 Concentration on Activated Carbon. *Sep. Sci. Technol.* 50, 1487–1496.  
 492 <https://doi.org/10.1080/01496395.2014.975360>
- 493 Delgado, L.F., Charles, P., Glucina, K., Morlay, C., 2012. The removal of endocrine disrupting compounds,  
 494 pharmaceutically activated compounds and cyanobacterial toxins during drinking water preparation  
 495 using activated carbon—A review. *Sci. Total Environ.* 435–436, 509–525.  
 496 <https://doi.org/10.1016/j.scitotenv.2012.07.046>
- 497 E Harrel Jr, F., 2017. Hmisc: Harrell Miscellaneous.
- 498 Ek, M., Baresel, C., Magnér, J., Bergström, R., Harding, M., 2014. Activated carbon for the removal of  
 499 pharmaceutical residues from treated wastewater. *Water Sci. Technol.* 69, 2372.  
 500 <https://doi.org/10.2166/wst.2014.172>
- 501 Ergun, S., Orning, A.A., 1949. Fluid Flow through Randomly Packed Columns and Fluidized Beds. *Ind. Eng.*  
 502 *Chem.* 41, 1179–1184. <https://doi.org/10.1021/ie50474a011>
- 503 Guillosoy, R., Le Roux, J., Mailler, R., Vulliet, E., Morlay, C., Nauleau, F., Gasperi, J., Rocher, V., 2019.  
 504 Organic micropollutants in a large wastewater treatment plant: What are the benefits of an advanced  
 505 treatment by activated carbon adsorption in comparison to conventional treatment? *Chemosphere* 218,  
 506 1050–1060. <https://doi.org/10.1016/j.chemosphere.2018.11.182>
- 507 Han, X., Wishart, E., Zheng, Y., 2014. A comparison of three methods to regenerate activated carbon saturated  
 508 by diesel fuels. *Can. J. Chem. Eng.* 92, 884–891. <https://doi.org/10.1002/cjce.21910>
- 509 Hsieh, C.-T., Teng, H., 2000. Influence of mesopore volume and adsorbate size on adsorption capacities of  
 510 activated carbons in aqueous solutions. *Carbon* 38, 863–869. [https://doi.org/10.1016/S0008-6223\(99\)00180-3](https://doi.org/10.1016/S0008-6223(99)00180-3)
- 512 Karanfil, T., Kilduff, J.E., Schlautman, M.A., Weber, W.J., 1996. Adsorption of Organic Macromolecules by  
 513 Granular Activated Carbon. 1. Influence of Molecular Properties Under Anoxic Solution Conditions.  
 514 *Environ. Sci. Technol.* 30, 2187–2194. <https://doi.org/10.1021/es9505863>
- 515 Li, L., Quinlivan, P.A., Knappe, D.R.U., 2002. Effects of activated carbon surface chemistry and pore structure  
 516 on the adsorption of organic contaminants from aqueous solution. *Carbon* 40, 2085–2100.  
 517 [https://doi.org/10.1016/S0008-6223\(02\)00069-6](https://doi.org/10.1016/S0008-6223(02)00069-6)
- 518 Li, Q., Snoeyink, V.L., Mariñas, B.J., Campos, C., 2003. Pore blockage effect of NOM on atrazine adsorption  
 519 kinetics of PAC: the roles of PAC pore size distribution and NOM molecular weight. *Water Res.* 37,  
 520 4863–4872. <https://doi.org/10.1016/j.watres.2003.08.018>
- 521 Liu, F., Zhao, J., Wang, S., Du, P., Xing, B., 2014. Effects of Solution Chemistry on Adsorption of Selected  
 522 Pharmaceuticals and Personal Care Products (PPCPs) by Graphenes and Carbon Nanotubes. *Environ.*  
 523 *Sci. Technol.* 48, 13197–13206. <https://doi.org/10.1021/es5034684>
- 524 Lussier, M.G., Shull, J.C., Miller, D.J., 1994. Activated carbon from cherry stones. *Carbon* 32, 1493–1498.
- 525 Mahajan, O.P., Moreno-Castilla, C., Walker Jr, P., 1980. Surface-treated activated carbon for removal of  
 526 phenol from water. *Sep. Sci. Technol.* 15, 1733–1752.
- 527 Mailler, R., Gasperi, J., Coquet, Y., Buleté, A., Vulliet, E., Deshayes, S., Zedek, S., Mirande-Bret, C., Eudes,  
 528 V., Bressy, A., Caupos, E., Moilleron, R., Chebbo, G., Rocher, V., 2016a. Removal of a wide range  
 529 of emerging pollutants from wastewater treatment plant discharges by micro-grain activated carbon

- 530 in fluidized bed as tertiary treatment at large pilot scale. *Sci. Total Environ.* 542, Part A, 983–996.  
531 <http://dx.doi.org/10.1016/j.scitotenv.2015.10.153>
- 532 Mailler, R., Gasperi, J., Coquet, Y., Derome, C., Buleté, A., Vulliet, E., Bressy, A., Varrault, G., Chebbo, G.,  
533 Rocher, V., 2016b. Removal of emerging micropollutants from wastewater by activated carbon  
534 adsorption: Experimental study of different activated carbons and factors influencing the adsorption  
535 of micropollutants in wastewater. *J. Environ. Chem. Eng.* 4, 1102–1109.  
536 <https://doi.org/10.1016/j.jece.2016.01.018>
- 537 Mailler, R., Gasperi, J., Coquet, Y., Deshayes, S., Zedek, S., Cren-Olivé, C., Cartiser, N., Eudes, V., Bressy,  
538 A., Caupos, E., Moilleron, R., Chebbo, G., Rocher, V., 2015. Study of a large scale powdered activated  
539 carbon pilot: Removals of a wide range of emerging and priority micropollutants from wastewater  
540 treatment plant effluents. *Water Res.* 72, 315–330. <https://doi.org/10.1016/j.watres.2014.10.047>
- 541 Margot, J., Kienle, C., Magnet, A., Weil, M., Rossi, L., de Alencastro, L.F., Abegglen, C., Thonney, D.,  
542 Chèvre, N., Schärer, M., Barry, D.A., 2013. Treatment of micropollutants in municipal wastewater:  
543 Ozone or powdered activated carbon? *Sci. Total Environ.* 461–462, 480–498.  
544 <https://doi.org/10.1016/j.scitotenv.2013.05.034>
- 545 Najm, I.N., Snoeyink, V.L., Richard, Y., 1991. Effect of Initial Concentration of a SOC in Natural Water on  
546 Its Adsorption by Activated Carbon. *J. - Am. Water Works Assoc.* 83, 57–63.  
547 <https://doi.org/10.1002/j.1551-8833.1991.tb07200.x>
- 548 Newcombe, G., 1994. Activated Carbon and Soluble Humic Substances: Adsorption, Desorption, and Surface  
549 Charge Effects. *J. Colloid Interface Sci.* 164, 452–462. <https://doi.org/10.1006/jcis.1994.1188>
- 550 Newcombe, G., Morrison, J., Hepplewhite, C., 2002a. Simultaneous adsorption of MIB and NOM onto  
551 activated carbon. I. Characterisation of the system and NOM adsorption. *Carbon* 40, 2135–2146.  
552 [https://doi.org/10.1016/S0008-6223\(02\)00097-0](https://doi.org/10.1016/S0008-6223(02)00097-0)
- 553 Newcombe, G., Morrison, J., Hepplewhite, C., Knappe, D.R.U., 2002b. Simultaneous adsorption of MIB and  
554 NOM onto activated carbon II. Competitive effects. *Carbon* 40, 2147–2156.
- 555 Paredes, L., Fernandez-Fontaina, E., Lema, J.M., Omil, F., Carballa, M., 2016. Understanding the fate of  
556 organic micropollutants in sand and granular activated carbon biofiltration systems. *Sci. Total*  
557 *Environ.* 551–552, 640–648. <https://doi.org/10.1016/j.scitotenv.2016.02.008>
- 558 Quinlivan, P.A., Li, L., Knappe, D.R.U., 2005. Effects of activated carbon characteristics on the simultaneous  
559 adsorption of aqueous organic micropollutants and natural organic matter. *Water Res.* 39, 1663–1673.  
560 <https://doi.org/10.1016/j.watres.2005.01.029>
- 561 R Core Team, 2007. R: A language and environment for statistical computing. R Foundation for Statistical  
562 Computing, Vienna, Austria.
- 563 Rafatullah, M., Sulaiman, O., Hashim, R., Ahmad, A., 2010. Adsorption of methylene blue on low-cost  
564 adsorbents: A review. *J. Hazard. Mater.* 177, 70–80. <https://doi.org/10.1016/j.jhazmat.2009.12.047>
- 565 Raposo, F., De La Rubia, M.A., Borja, R., 2009. Methylene blue number as useful indicator to evaluate the  
566 adsorptive capacity of granular activated carbon in batch mode: Influence of adsorbate/adsorbent mass  
567 ratio and particle size. *J. Hazard. Mater.* 165, 291–299. <https://doi.org/10.1016/j.jhazmat.2008.09.106>
- 568 Shi, B., Fang, L., Li, Z., Wang, D., 2014. Adsorption Behavior of DOM by PACs with Different Particle Sizes.  
569 *CLEAN – Soil Air Water* 42, 1363–1369. <https://doi.org/10.1002/clen.201300518>
- 570 Streicher, J., Ruhl, A.S., Gnirß, R., Jekel, M., 2016. Where to dose powdered activated carbon in a wastewater  
571 treatment plant for organic micro-pollutant removal. *Chemosphere* 156, 88–94.  
572 <https://doi.org/10.1016/j.chemosphere.2016.04.123>
- 573 Tran, H.N., Wang, Y.-F., You, S.-J., Chao, H.-P., 2017. Insights into the mechanism of cationic dye adsorption  
574 on activated charcoal: The importance of  $\pi$ - $\pi$  interactions. *Process Saf. Environ. Prot.* 107, 168–180.  
575 <https://doi.org/10.1016/j.psep.2017.02.010>
- 576 Vulliet, E., Cren-Olivé, C., Grenier-Loustalot, M.-F., 2011. Occurrence of pharmaceuticals and hormones in  
577 drinking water treated from surface waters. *Environ. Chem. Lett.* 9, 103–114.  
578 <https://doi.org/10.1007/s10311-009-0253-7>

- 579 Wang, S., Zhu, Z.H., Coomes, A., Haghseresht, F., Lu, G.Q., 2005. The physical and surface chemical  
580 characteristics of activated carbons and the adsorption of methylene blue from wastewater. *J. Colloid*  
581 *Interface Sci.* 284, 440–446. <https://doi.org/10.1016/j.jcis.2004.10.050>
- 582 Yu, J., Lv, L., Lan, P., Zhang, S., Pan, B., Zhang, W., 2012. Effect of effluent organic matter on the adsorption  
583 of perfluorinated compounds onto activated carbon. *J. Hazard. Mater.* 225, 99–106.  
584 <https://doi.org/10.1016/j.jhazmat.2012.04.073>
- 585 Yu, Z., Peldszus, S., Huck, P.M., 2008. Adsorption characteristics of selected pharmaceuticals and an  
586 endocrine disrupting compound—Naproxen, carbamazepine and nonylphenol—on activated carbon.  
587 *Water Res.* 42, 2873–2882. <https://doi.org/10.1016/j.watres.2008.02.020>
- 588 Zietzschmann, F., Altmann, J., Ruhl, A.S., Dünnbier, U., Dommisch, I., Sperlich, A., Meinel, F., Jekel, M.,  
589 2014. Estimating organic micro-pollutant removal potential of activated carbons using UV absorption  
590 and carbon characteristics. *Water Res.* 56, 48–55. <https://doi.org/10.1016/j.watres.2014.02.044>
- 591 Ziska, A.D., Park, M., Anumol, T., Snyder, S.A., 2016. Predicting trace organic compound attenuation with  
592 spectroscopic parameters in powdered activated carbon processes. *Chemosphere* 156, 163–171.  
593 <https://doi.org/10.1016/j.chemosphere.2016.04.073>  
594